DOI: 10.24850/j-tyca-14-02-04
Articles

# Validation and correction of satellite-estimated precipitation using ground observations in the Pampean region of Argentina

# Validación y corrección de estimaciones de precipitación satelital utilizando observaciones en superficie en la región pampeana argentina

Martin Blanco[1], ORCID: https://orcid.org/0000-0002-3461-3484
Eleonora Demaria[2], ORCID: https://orcid.org/0000-0003-3051-1058
Georgina Cazenave[3]
Erik Zimmermann[4]

[1]Instituto de Hidrología de Llanuras "Dr. Eduardo Jorge Usunoff" (IHLLA), Buenos Aires, Argentina / Consejo Nacional de Investigaciones Científicas y Técnicas (CONICET), martinblanco@ihlla.org.ar
[2]Pima County Regional Flood Control District, Tucson, AZ, USA, eleonora.demaria@pima.gov
[3]Instituto de Hidrología de Llanuras "Dr. Eduardo Jorge Usunoff" (IHLLA), Buenos Aires, Argentina, cazenave@ihlla.org.ar

[4]Consejo Nacional de Investigaciones Científicas y Técnicas (CONICET) / Universidad Nacional de Rosario, Facultad de Ciencias Exactas Ingeniería y Agrimensura (UNR), Rosario, Argentina, erikz@fceia.unr.edu.ar

Corresponding author: Martin Blanco, martinblanco@ihlla.org.ar

**Abstract**

Satellite-estimated precipitation represent an alternative source of information for different hydrological applications, hence understanding the skill of satellite products to capture the spatial and temporal variability of precipitation is crucial for the development of hydrometeorological monitoring and early warning systems. This study evaluates the reliability of three satellite precipitation products (SPP) in the Pampean region of Argentina, before and after applying the Quantile Mapping bias correction method. The SPP used are TMPA, CMORPH and IMERG in their near real time versions. The evaluation was carried out using categorical and descriptive statistics in order to assess their skills to provide reliable estimates and correctly detect the magnitude of precipitation events. The categorical statistical analysis was carried out at a daily time step, in this case SPPs better estimate the observations for low intensities (less than 5 mm) and medium (between 5 and 20 mm) than for high intensities (greater than 20 mm). The evaluation of the descriptive statistics at the monthly level showed that the CMORPH has the highest detection skill in

the EFM and AMJ quarters, while the IMERG obtained the lowest errors for the JAS and OND quarters. The incorporation of a bias removal method in the SPP validation process introduced significant improvements in the evaluated statistics. Especially the CMORPH which significantly improved its performance when compared with the IMERG, being the TMPA the one showing the larger errors in the region.

**Keywords**: Satellite precipitation products, near real time, bias correction, validation.

## Resumen

Las estimaciones de precipitación basadas en satélites representan una valiosa fuente de información alternativa para diferentes aplicaciones hidrológicas, por lo que entender la habilidad de los productos satelitales para capturar la variabilidad espacial y temporal de la precipitación es crucial para el desarrollo de sistemas de monitoreo y alerta hidrometeorológica. En este trabajo se evalúa la confiabilidad de tres productos de precipitación satelital (PPS) en la región pampeana argentina, antes y después de aplicarles el método de corrección de sesgo Quantile Mapping. Los PPS usados son TMPA, CMORPH e IMERG, todos en sus versiones en tiempo casi real. La evaluación se realizó mediante estadísticos categóricos y descriptivos a fin de conocer su capacidad en proporcionar estimaciones confiables y detectar correctamente la magnitud de los eventos. El análisis de los estadísticos categóricos se

realizó a nivel diario; en este caso, los PPS estiman mejor las observaciones para intensidades bajas (menores a 5 mm) y medias (entre 5 y 20 mm) que para intensidades altas (mayores a 20 mm). La evaluación de estadísticos descriptivos a nivel mensual mostró que el CMORPH tiene mayor capacidad de detección en los trimestres EFM y AMJ, mientras que el IMERG obtuvo los menores errores para los trimestres JAS y OND. La incorporación de un método de remoción del sesgo en el proceso de validación de los PPS introdujo mejoras significativas en los estadísticos evaluados. Especialmente el CMORPH superó su rendimiento al compararlo con el IMERG, siendo el TMPA el que mayores errores presenta en la región.

**Palabras clave**: productos de precipitación satelital, tiempo casi real, corrección de sesgos, validación.

Received: 07/15/2021

Accepted: 09/29/2021

# Introduction

Precipitation is the most important climatic variable of the hydrological system, so understanding its spatial and temporal behavior is necessary both for the development of hydrometeorological monitoring and warning systems, as well as for decision-making in the areas of meteorology, hydrology, and agriculture. Historically, precipitation is observed in surface weather stations, which provide direct measurements, but are generally not evenly distributed and are subject to errors associated with the type of precipitation, wind, lack of maintenance, among other factors. It was in the seventies when the first techniques were developed to estimate precipitation from radiometric satellite observations. Initially, precipitation was estimated with visible or infrared wavelength sensors, through the reflectivity and temperature of the cloud top. Subsequently, the introduction of passive microwave sensors that penetrate clouds and measure the size of raindrops allowed a decrease in uncertainty in estimated precipitation (Ebert, Janowiak, & Kidd, 2007).

In recent years, various satellite precipitation products (SPP) have been developed, using different techniques to estimate precipitation based on the combined information of several satellites, among which we can mention the TRMM Multi-satellite Precipitation Analysis (TMPA) of the Tropical Rainfall Measuring Mission (TRMM) (Huffman *et al*., 2007), the product Climate Prediction Center (CPC) Morphing Technique Product

(CMORPH) (Joyce, Janowiak, Arkin, & Xie, 200), and the Integrated Multi-Satellite Retrievals for GPM (IMERG) esteemed with the mission of Global Precipitation Measurement (GPM) (Huffman *et al*., 2014).

Typically, satellites cannot offer the same detail on a timescale with fast upgrades as weather stations with real-time transmission. But satellite coverage has numerous advantages that make its uses attractive for different disciplines. In this sense, it can be mentioned that SPP are systematically available worldwide, have continuous measurement, provide spatially uniform data with wide spatial resolution that includes the vast ocean areas, can be downloaded for free and some products have availability near real time. However, SPP also have some limitations, as evidenced by different assessments with surface observations made in various geographical regions (Hong, Hsu, Moradkhani, & Sorooshian, 2006; Hossain & Anagnostou, 2004; Hossain & Anagnostou, 2006; Iida, Kubota, Iguchi, & Oki, 2010; Tang, Hossain, & Huffman,2010; Tang & Hossain, 2009; Yilmaz *et al*., 2005). These studies point out important biases in SPP due to different sources of uncertainty, such as sampling errors due to spatial and temporal discontinuity of measurements and/or calibration problems in satellite sensors.

In addition, there are other factors that can influence SPP errors such as the precipitation regime or the topography of each particular region. Zambrano-Bigiarini, Nauditt, Birkel, Verbist and Ribbe (2017) evaluated seven SPP in Chile and showed that the adjustment with the

observations was greater in humid areas with low and medium elevations (0-1 000 masl) than in the arid regions of the north and the extreme south. These results indicate that SPP should be evaluated in terms of error with surface observations since their performance could vary according to their geographical location as evidenced by various studies conducted in different parts of the world (Aslami, Ghorbani, Sobhani, & Esmali, 2019; Basheer & Elagib, 2019; Gella, 2019; Tan & Duan, 2017; Tan & Santo, 2018). Particularly in South America, SPP analyses have yielded mixed results (Baez-Villanueva *et al*., 2018; Dinku, Ruiz, Connor, & Ceccato, 2010; Melo *et al*., 2015; Oreggioni-Weiberlen & Báez-Benítez, 2018; Palharini *et al*., 2020; Zambrano-Bigiarini *et al*., 2017). Bias in SPP was recognized as a relevant problem in several basins around the world, and bias correction methods were shown to significantly reduce errors in simulated flows (Maggioni & Massari, 2018).

Hobouchian, Salio, García-Skabar, Vila and Garreaud (2017) conducted a validation of four estimates of daily precipitation by satellite over the subtropical Andes. Their results indicate a decrease in errors in the winter season that coincides with the rainy season. Both this analysis and the validation of six SPP carried out in southern South America by Salio, Hobouchian, García-Skabar and Vila (2015) highlight that the estimates that include microwave information capture precipitation better than those that do not consider them. They also demonstrated that the products with less bias are those that are calibrated with surface

observations such as TMPA (3B42). However, these have a limitation for their use since they are only available after 2 months of publishing their version without correction.

The Pampean region is an area with typical plain characteristics, consequently it is a vulnerable environment to extreme hydrological events, both water deficit and water excess. Faced with situations of excess, the low topographic slope together with other factors prevents the outflow of important volumes of water, therefore long lasting floods usually occur in a significant fraction of the landscape (Aragón, Jobbágy, & Viglizzo, 2011). The plains of Argentina have a great socio-economic preponderance since they stand out for their great extension and for the quality of their lands, which makes them one of the main regions of the world in the production of wheat, corn and soybeans, and cattle breeding. This pressure to be productive, along with the lack of flood warning and monitoring systems, makes them very vulnerable systems, which motivated the choice of SPP near real time for evaluation in the present work.

The objectives of this work are: 1) to evaluate the ability to detect frequencies and magnitudes of daily and seasonly precipitation of three SPP in their version near real time, using surface rainfall observations in a plain area; 2) to select the SPP that best represents the space-time variability of precipitation in the region; and 3) to estimate the impact of bias removal between SPP and surface observations.

# Data

## Study area

The Pampean region is in east-central Argentina, in South America. It comprises the southern provinces of Entre Ríos and Santa Fe, the southeast of Córdoba, the northeast of La Pampa, part of San Luis and most of the province of Buenos Aires (Figure 1). It is an extensive plain, covering an area of approximately 600 000 $km^2$ (Aliaga, Ferrelli, & Piccolo, 2017). The economy is mainly based on agricultural-livestock production and industrialization being the most productive rainfed area in the country, concentrating more than 90 % of soybean production and between 80 and 90 % of wheat, corn, sorghum, barley and sunflower production (Magrin, Travasso, López, Rodriguez, & Lloveras, 2007).



*Tecnología y ciencias del agua*, ISSN 2007-2422, 14(2), 110-168. DOI: 10.24850/j-tyca-14-02-04

Tecnología y Ciencias del Agua

OPEN ACCESS

Check for updates

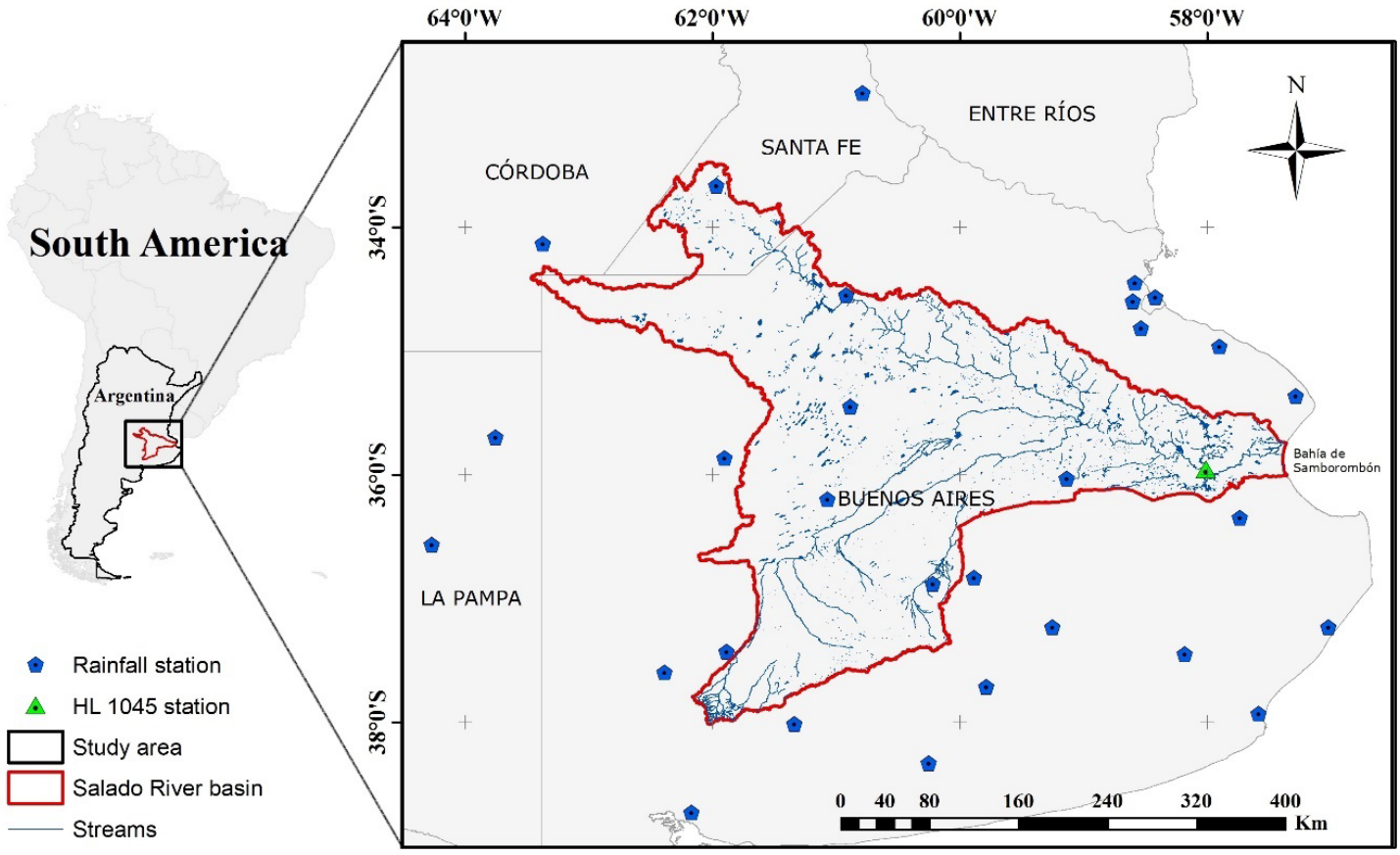


**Figure 1**. Location of the study area and the rainfall stations on the surface.

The main characteristic of the Pampean region is its flat relief, consisting of a plain of low topographic gradient (slopes < 0.1 %),

elevations less than 200 masl and poorly developed drainage networks. In wet seasons this low morphology conditions the formation of temporary floods, waterlogging of the soil, accumulation of salts near the surface and development of marshes and shallow ponds (Fuschini-Mejía, 1994).

One of the main water systems in the Pampean region is the Salado River basin, which covers an area of approximately 90,000 $km^2$ and is located mainly in the Province of Buenos Aires. The Salado River basin has its headwaters southeast of the province of Córdoba and southwest of Santa Fe, flows into the bay of Samborombón in the Atlantic Ocean (Figure 1) and has an average daily flow of 210 m3 / s recorded in the HL 1045 station for the period 1990-1998. During periods of excess water, extreme flows have been observed, such as floods in December 1985 (1 454 $m^3/s$), July 1993 (1 380 $m^3/s$) and April 2002 (1 429 $m^3/s$).

The selected study area is limited by the meridians 56° 30' W and 64° 30' W and the parallels 32° 30' S and 39° 00' S (Figure 1) and comprises the Salado River basin. The climate is humid temperate, the average annual temperature is 16°C with an average maximum in January of 24°C and minimum in June of 9°C. The average annual rainfall is about 1 050 mm in the northeast gradually decreasing to about 650 mm to the southwest. This region has different precipitation regimes between the warm and cold seasons. Whereas during the winter months (June, July and August) precipitation is associated with cold fronts that cause low intensity rainfall and large spatial extension, during the spring

months (October, November and December) and summer (January, February and March) precipitation is frequently associated with the presence of warm fronts and the so-called air mass storms characterized by heavy rainfall of convective origin.

## Surface rainfall stations

Rainfall information was collected from 29 surface stations, belonging to the National Meteorological Service (SMN) and the National Institute of Agricultural Technology (INTA, *Instituto Nacional de Tecnología Agropecuaria*), located in the province of Buenos Aires, south of Santa Fe, south of Córdoba and east of La Pampa as shown in Figure 1. The data measured by the stations are known as the accumulated daily precipitation (called Observed Data for this analysis) at 12:00 UTC (9:00 AM local time).

## Satellite precipitation products

The National Aeronautics and Space Administration (NASA) and the Japan Aerospace Exploration Agency (JAXA), in 1997 launched the TRMM satellite designed to monitor and study tropical rainfall. It has five sensors on board, of which three are for rain measurement: a precipitation radar (PR) that provides data on intensity, distribution and type of rain; a passive microwave imaging sensor (TMI) that quantifies water vapor, water in clouds and rainfall intensity; and a visible and infrared scanner (VIRS), being the principle of observation and the bandwidth of each different: 760, 720 and 215 km respectively. The information recorded by these sensors is published by NASA.

For this work, data from real-time TRMM multisatellite precipitation analysis (Huffman *et al*., 2007) version 7 were used. The product used is the 3B42RT (from now on it will be called TMPA) that has a global coverage from 60° north to 60° south, its spatial resolution is 0.25° and temporary 3 hours. The archives are publicly accessible and have been available since March 2000, although they do not include calibration measurements using surface rainfall observations such as product 3B42, precipitation estimates are available with a delay of approximately 8 hours, which is suitable for near real-time monitoring and modeling activities.

The CMORPH precipitation estimation algorithm was developed in the United States by the National Oceanic and Atmospheric Administration (NOAA). Precipitation estimates are based solely on data from passive microwave sensors (Joyce *et al*., 2004) and IR images are not used to estimate precipitation but only to interpolate between two fields of rainfall intensity derived from microwave sensors. The precipitation product that was used in this work was CMORPH in its versions 1.0 (for the period 2001-2014) and subsequently version 0.x was used until December 2017. The data in this product has the same coverage, spatial and temporal resolution as the TMPA product.

The GPM mission is an international network of satellites that provides global rainfall observations that is built upon the basis of the success of the TRMM mission. The IMERG algorithm combines information from the GPM satellite constellation to estimate precipitation over most of the Earth's surface. In the latest version v.6 (Huffman *et al*., 2019) the algorithm merges the early precipitation estimates collected during the operation of the TRMM satellite (2000-2015) with more recent precipitation estimates collected during the operation of the GPM satellite (2014-present).

The IMERG offers three different types of products, the "Final" product that is available 3.5 months after the observation period, the "Late" product available after 14 hours and the "Early" product that is available only 4 hours after its observation time. This last product is the

one used in the present work, and has a spatial distribution of 0.1° x 0.1°, temporary of 30 minutes and global coverage from 90° north to 90° south.

# Methodology

## Evaluation of SPPs

To properly assess the precipitation between the SPP and the observed data it is necessary to consider the spatial scale mismatch between them. SPP are available at grid or pixel scale (0.1° for the IMERG product and 0.25° for the CMORPH and TMPA products), while the observed data represents point precipitation.

In this study the evaluation was carried out on two different spatial scales: 1) pixel (SPP) *versus* point (observed data), and 2) pixel (SPP) *versus* pixel (observed data). The first scale enables to evaluate the

behavior of the nearest pixel of the SPP with respect to each rainfall station (observed data); in this case a daily temporal resolution was used. Whereas the second scale enables to evaluate the behavior of the SPP in a distributed way in the study area, for this evaluation to be possible it was necessary to perform an interpolation of the observed data and a resampling of the data of the IMERG product so that the size of the pixel is compatible (0.25°); the temporal resolution used was monthly.

Some researchers (Borges, Franke, Da-Anunciação, Weiss, & Bernhofer, 2016; Cisneros-Iturbe, Bouvier, & Domínguez-Mora, 2001) have argued that interpolation is likely to produce some uncertainty associated with the calculation method or the density of the measuring stations. On the other hand, the spatial sampling error decreases with increasing the time of accumulation of precipitation (Maggioni & Massari, 2018; Villarini, Mandapaka, Krajewski, & Moore, 2008). For this reason and in order to minimize these errors in the spatial scale pixel *versus* pixel was evaluated with a monthly temporal resolution.

The evaluation of the different products was carried out in two ways: applying categorical statistics that allow evaluating the capacity of detection of the precipitation of the SPP with respect to the observed data, and the descriptive statistics that allow knowing quantitatively the errors and correlations that exist between the observed data and the SPP.

Categorical statistics were used considering the different precipitation thresholds (0.5, 1, 2, 3, 4, 5, 10, 15, 20, 25, 30, 35, 40, 45

and 50 mm/day). Each event was classified as proposed by Ebert *et al*. (2007) using the following categories: success (H, the observed precipitation and the SPP are above the threshold), surprise (M, the observed precipitation is above the threshold and that of the SPP below) and false alarm (F, the precipitation of the SPP is above the threshold and that observed below).

The categorical statistics applied are the Bias Score (BIASS), the Probability of Detection (POD), the False Alarm Ratio (FAR) and the Equitable Threat Score (ETS), their formulas are presented in Table 1. BIASS is the relationship between the number of estimated precipitation events and the number of precipitation events observed, which indicates whether the estimated precipitation has a tendency to underestimate (BIASS < 1) or overestimate (BIASS > 1), but does not provide a measure of that magnitude (it only measures relative frequencies); the POD shows what fraction of observed events was captured correctly (sensitive to hits but ignores false alarms); the FAR shows the fraction of the events estimated by the SPP that did not actually occur (sensitive to false alarms but ignores surprises); and the ETS calculates the correctly estimated precipitation fraction considering the number of random hits.

Tecnología y Ciencias del Agua

OPEN ACCESS

Check for updates

**Table 1**. Categorical statistics used in the evaluation of SPP. H: observed precipitation and SPP are above the threshold; M: the observed precipitation is above the threshold and that of the SPP below; F: SPP precipitation is above the threshold and observed below; T represents the total number of events.

| Index | Equation | Ideal value |
|---|---|---|
| Bias score | $BIASS = \frac{H+F}{H+M}$ | 1 |
| Probability of Detection | $POD = \frac{H}{H+M}$ | 1 |
| False Alarm Ratio | $FAR = \frac{F}{H+F}$ | 0 |
| Equitable Threat Score | $ETS = \frac{H - \frac{(H+M).(H+F)}{T}}{H+M+F-\frac{(H+M).(H+F)}{T}}$ | 1 |

The second method consisted of the application of descriptive statistics to quantify the magnitude of errors between surface observations and SPP. In addition to using the point *versus* pixel ratio with daily temporal resolution, the pixel *versus* pixel ratio at a monthly temporal resolution was also used. For this last relationship to be possible, it was necessary to make a spatial distribution of the observed precipitation data. This spatial distribution was carried out with the

Inverse Distance Weighting (IDW) method, using Geographic Information Systems tools.

The IDW method has a long history of use and reliability, mainly due to its simplicity in formulation and its wide application in operating environments, it is frequently used to interpolate precipitation (Campozano, Sánchez, Avilés, & Samaniego, 2014; Guevara-Ochoa *et al*., 2017; Kim & Ryu, 2016). With this method, the estimated value is obtained through a weighted average of all values that are within a search area. The method assigns the greatest weight to the nearest point, which decreases as the distance increases. Its equation is expressed as:

$$W_p = \frac{\sum_{i=1}^{n} \frac{W_i}{(d_i)^{\beta}}}{\sum_{i=1}^{n} \left(\frac{1}{d_i}\right)^{\beta}} \qquad (1)$$

where:$W_p$ is the estimated value at point p; $n$ is the number of points used in interpolation; $W_i$is the value known in it $i$-th point; $d_i$ is the distance from the known point $i$ to the point to be estimated $p$; and $\beta$ is the power of the inverse of the distance.

To evaluate the performance of the SPP and compare them with surface precipitation data, different descriptive statistics were used (Aslami *et al*., 2019; Tan & Duan, 2017). The Pearson correlation coefficient (R) was used to assess the extent of the agreement between

the SPP and the observed data, which varies between -1 and 1. The root mean square error (RMSE) represents the standard deviation of the sample of the differences between the estimated values and the observed values. Statistical bias (BIAS) is the average difference between the SPP and the observed data; this statistic was used to estimate the percentage of underestimation or overestimation between the variables. In addition, to evaluate the efficiency of the product, the Nash-Sutcliffe index (NSE) was calculated. This index ranges between -∞ and 1 (Table 2).

**Table 2**. Descriptive statistics used in the evaluation of SPP. $m$ sample size; $Sn$: satellite precipitation estimates; $On$: surface observations; $\tilde{S}$: arithmetic mean of satellite precipitation estimates; $\tilde{O}$: arithmetic mean of surface observations.

| Statistical metric | Equation | Ideal value |
|---|---|---|
| Pearson correlation coefficient | $R = \frac{\sum_{k=1}^{m}(Sn-\tilde{S})(On-\tilde{O})}{\sqrt{\sum_{k=1}^{m}(Sn-\tilde{S})^2}\sqrt{\sum_{k=1}^{m}(On-\tilde{O})^2}}$ | 1 |
| Root mean square error | $RMSE = \sqrt{\frac{1}{m}\sum_{k=1}^{m}(Sn-On)^2}$ | 0 |
| Statistical bias | $BIAS = \frac{\sum_{k=1}^{m}(Sn-On)}{\sum_{k=1}^{m}On} \times 100$ | 0 |
| Nash-Sutcliffe index | $NSE = 1 - \frac{\sum_{k=1}^{m}(On-Sn)^2}{\left(\sum_{k=1}^{m}(On-\tilde{O})^2\right)}$ | 1 |

Tecnología y Ciencias del Agua

OPEN ACCESS

Check for updates

# Bias correction of SPPs

After evaluating the SPP with respect to the observed data, the bias correction method was applied. The procedure used is Quantile Mapping (QM), which is a non-parametric method (Fang, Yan, Chen, & Zammit, 2015) that consists of implementing statistical transformations to correct the bias of SPP. This approach is based on the ratio of quantiles which converges the empirical cumulative distribution function for probability of the simulated variables to those observed. Some authors have successfully used this method for the correction of precipitation and temperature bias in global and regional climate models (Heo, Ahn, Shin, Kjeldsen, & Jeong, 2019; Ines & Hansen, 2006; Luo *et al*., 2018; Themeßl, Gobiet, & Heinrich, 2012).

Bias correction was performed by constructing the monthly cumulative distribution functions of the SPP and the observed data using a transfer function that allows the uncorrected SPP to be transferred to corrected SPP. Therefore, the cumulative distribution function of the SPP is transformed to match the observed data set. Figure 2 shows a

description of the QM method used in this work. The equation used for bias correction is as follows:

$$P_c = F_o^{-1}(F_s(P_s)) \quad (2)$$

where: $P_c$ is the value of the corrected SPP; $P_s$ is the value of the SPP to be corrected; $F_o^{-1}$ is the inverse of the cumulative distribution function of the observed data; and $F_s$ is the cumulative distribution function of the SPP used.

Tecnología y Ciencias del Agua
OPEN ACCESS
Check for updates

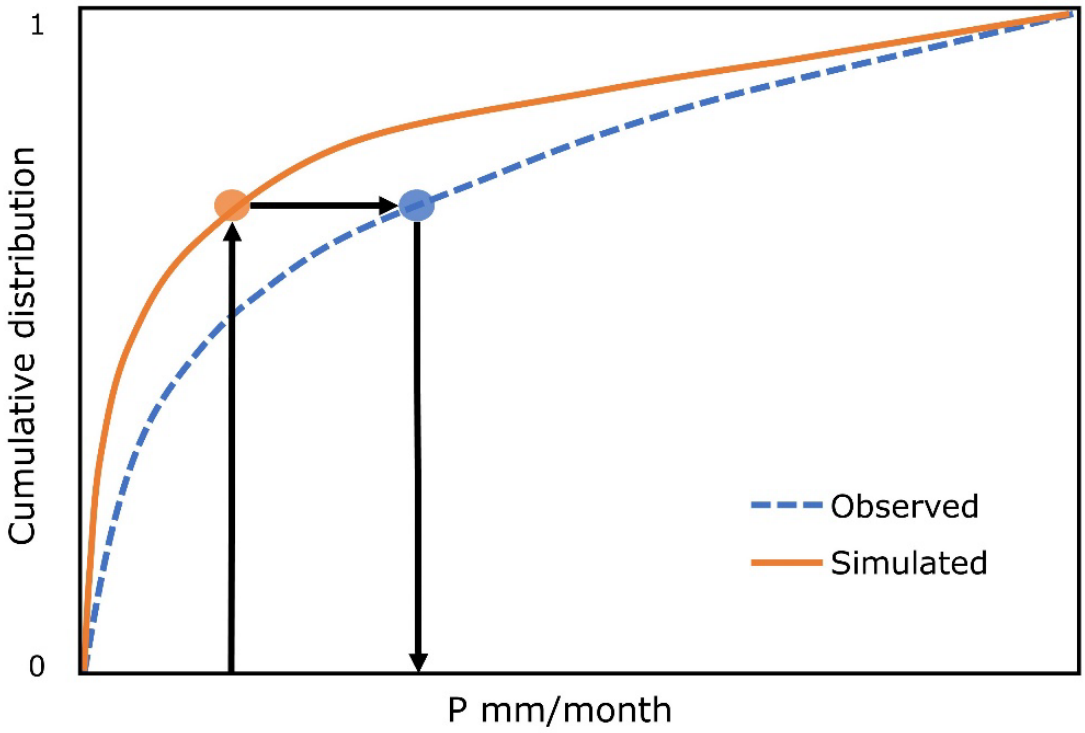


**Figure 2**. Graphical representation of the QM method.

The QM method was applied to monthly precipitation distributions and the relationship between SPP and corrected SPP was used to temporarily disaggregate corrected data from monthly to daily level.

After the application of bias correction to the SPP, the calculation of the descriptive statistics was updated. The evaluation of SPP was performed for both spatial scales (point *versus* pixel and pixel *versus* pixel), then the products were compared in their corrected and

uncorrected versions. To differentiate the SPP from the corrected SPP, -C was added to the end of each product name. Figure 3 shows an outline of the methodology described in Figure 3.

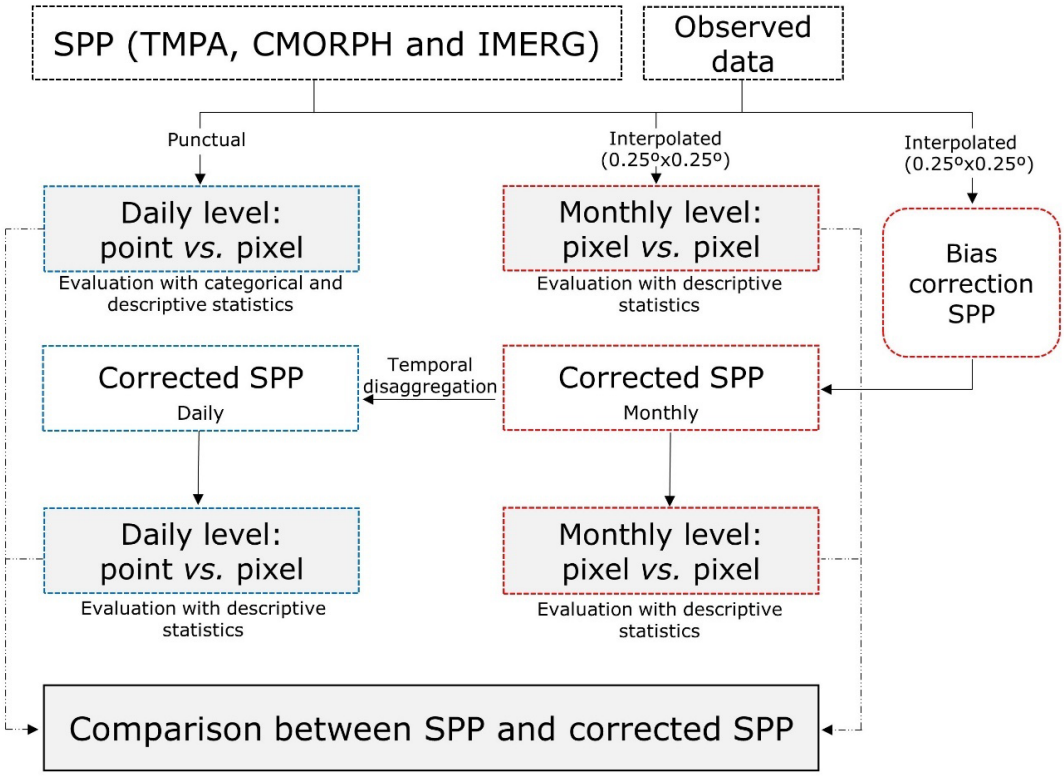


**Figure 3**. Outline of the methodology.

# Results

## Temporal and spatial variability analysis of precipitation

Figure 4 shows the average monthly rainfall for the study region, the maximum and minimum are referred to the different seasons, considering the average rainfall in each one. The results show that 65 % of the precipitation occurs between the months of October to March, where the influence of the South Atlantic anticyclone leads to a warm and humid air mass that generates copious precipitation. This effect decreases markedly in the coldest months from April to September, when the anticyclone moves north limiting the entrance of humid air masses. In relation to the average rainfall, the lowest values occur in the month of June with 33 mm, the presence of two annual maximum values is also observed, the main one in the month of February with 116 mm and the second in the month of October with 105 mm.



*Tecnología y ciencias del agua*, ISSN 2007-2422, 14(2), 110-168. DOI: 10.24850/j-tyca-14-02-04

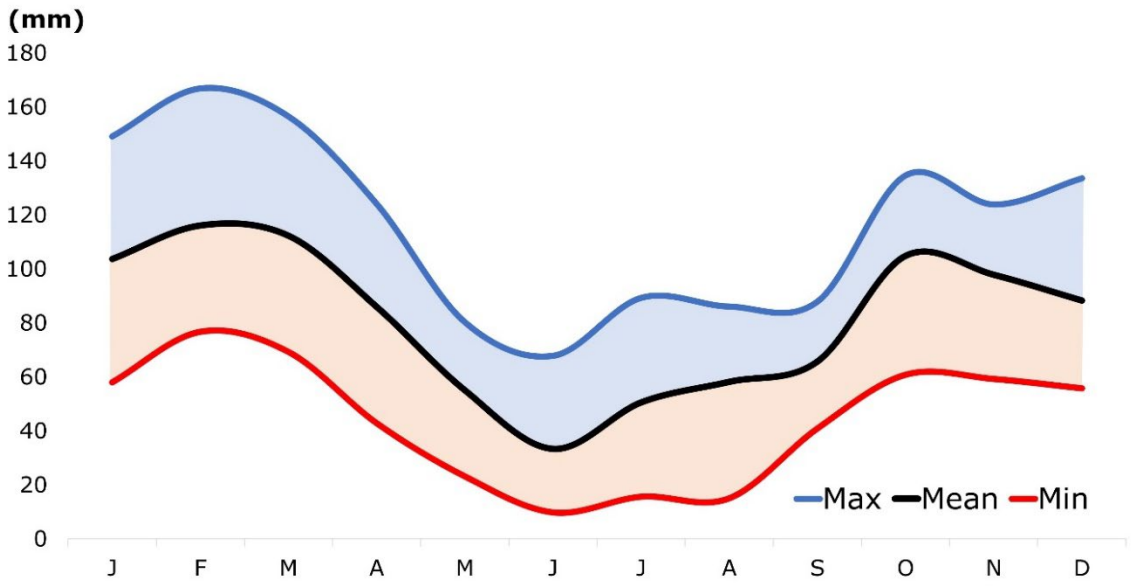


**Figure 4**. Monthly average precipitation for surface rainfall seasons. Period 2001–2017.

Figure 5 shows how the space-time distribution of precipitation varies depending on the proximity of surface stations to the Atlantic Ocean. For example, the Rosario Aero, Laboulaye Aero and Santa Rosa Aero stations are in the continental zone of influence, where there is a more marked seasonality with 75 % of precipitation occurring in the warm semester (October to March). This marked seasonal variation is due to the source of water vapor from the center-north of the country to a warmer surface, which favors the formation of precipitation of convective origin during this period. In contrast, the stations La Plata Aero, Azul Aero,

Bahía Blanca Aero and Mar del Plata Aero are within the area with maritime influence in which a less marked seasonality is reflected with 60 % of the precipitation in the same months.

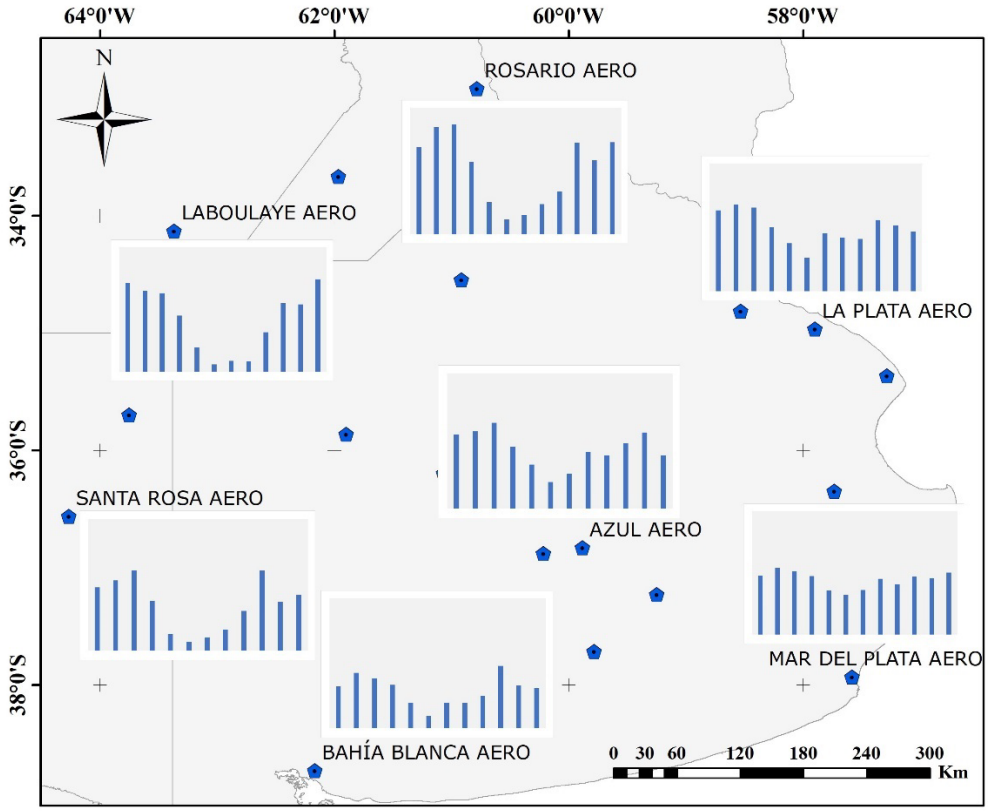


**Figure 5**. Geographical location of the rainfall seasons on the surface and seasonal precipitation regime. Period 2001-2017.

In the spatial distribution of annual precipitation (Figure 6a) there is a decreasing trend that goes from the northeast with values higher than 1 050 mm / year to the southwest with values below 650 mm / year. The three SPPs presented in Figure 6 (b, c and d) follow the same spatial distribution pattern as the observed precipitation. However, all products have a tendency to overestimate precipitation, the most evident being the IMERG product with values higher than 2 000 mm / year in the northeast part of the region and minimum values close to 1 000 mm / year in the southwest.

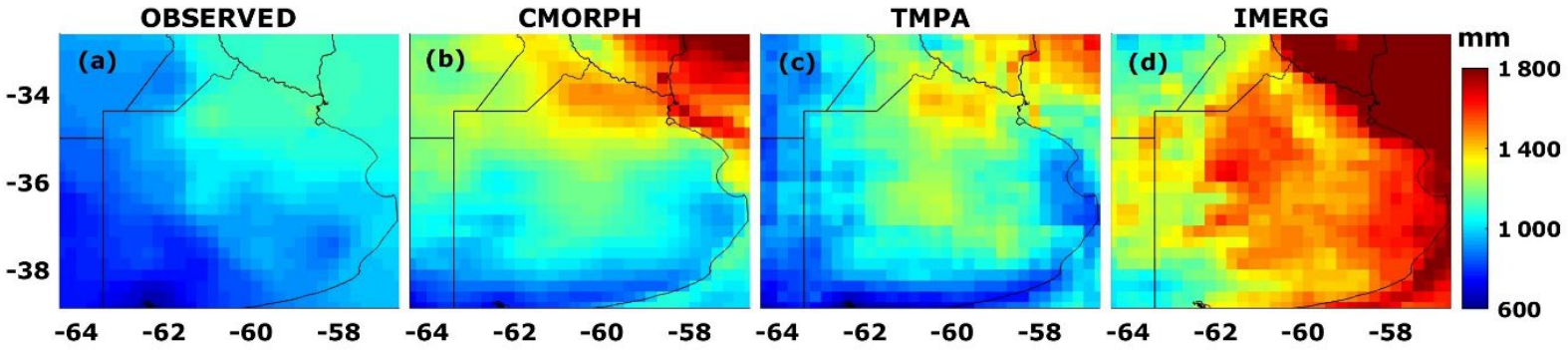


**Figure 6**. Spatial distribution of the precipitation observed and estimated by the different SPP (mm/year). Period 2001-2017.

When comparing the average seasonly precipitation of the SPPs with the data observed on the surface (Figure 7), it can be seen that these capture the spatial variability but not the magnitude of the precipitation

in the region. The accumulated precipitation in the weather stations was greater in JFM and OND, for these cases the average was 330 mm and 295 mm respectively. In these two seasons the SPP overestimate the precipitation observed in almost the entire study area, being more noticeable this difference in the IMERG product, for which an average value of 530 mm (JFM) and 440 mm (OND) was obtained, followed by the CMORPH product with an average of 485 mm (JFM) and 405 mm (OND). Finally, the TMPA showed results closer to those observed with average values of 398 mm (JFM) and 327 mm (OND). On the other hand, the accumulated precipitation in the weather stations was lower in AMJ and JAS for which values of 166 mm and 162 mm correspond. During these season seasonal in the west of the region the three SPP show an underestimation of precipitation, while in the east they tend to overestimate it. Specifically, in JAS the products CMORPH and TMPA underestimated the precipitation with average values of 146 mm and 135 mm respectively, in turn, in AMJ the only product that underestimates is the CMORPH for which an average of 163 mm was obtained.

Tecnología y Ciencias del Agua

OPEN ACCESS

Check for updates

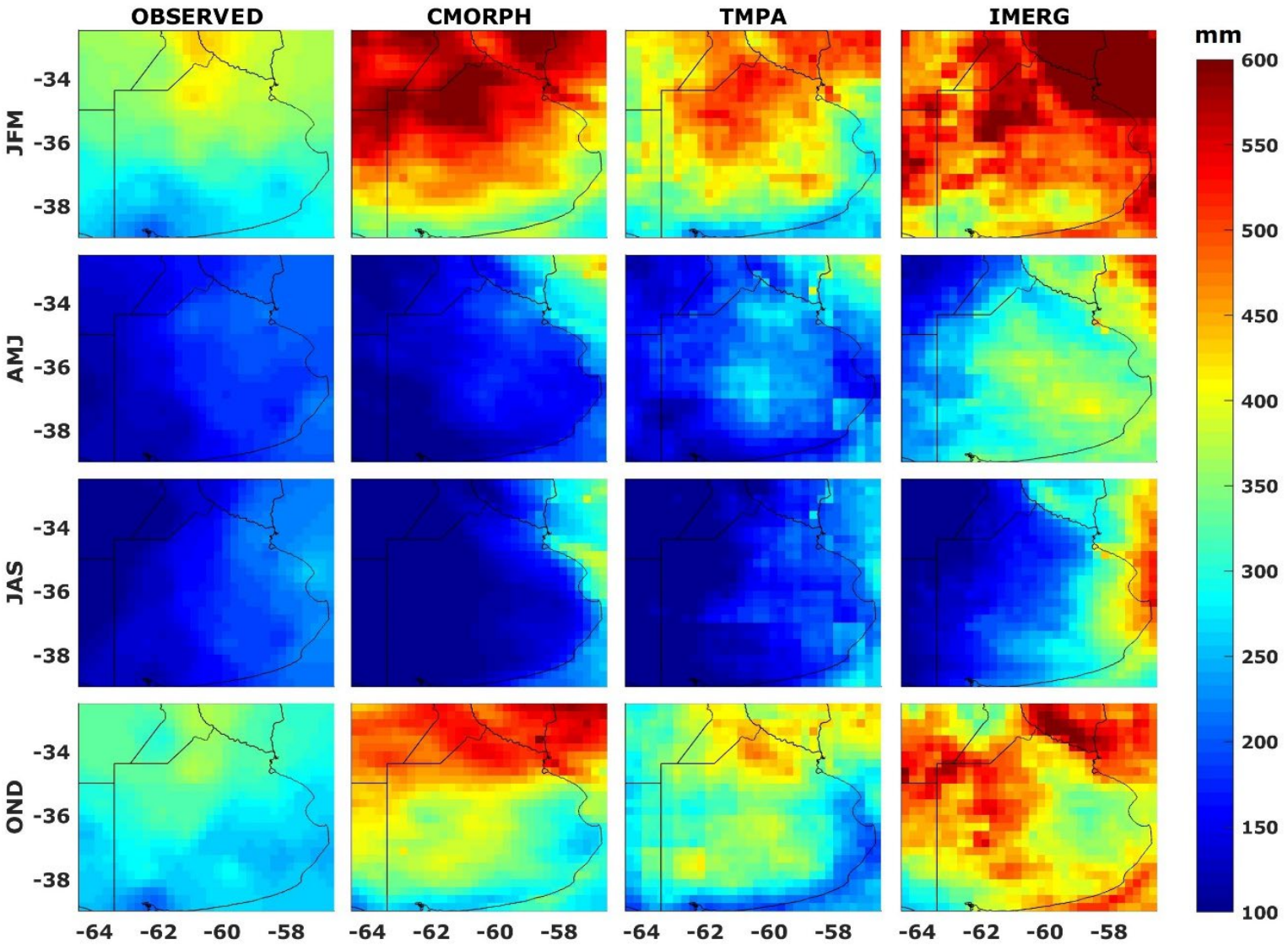


**Figure 7**. Spatial distribution of season seasonal average precipitation in mm. Period 2001-2017.

Tecnología y Ciencias del Agua

OPEN ACCESS

Check for updates

## SPP assessment

### Daily level: point *vs*. pixel

The POD, FAR, BIASS and ETS statistical coefficients (Table 1) show that SPP captures observations for low (up to 5 mm) and medium (between 5 and 20 mm) rainfall intensities. While for high intensities (greater than 20 mm), the BIASS is greater than 1 for all SPPs, which indicates an overestimation in this type of event, with the TMPA being the one that best represents the intense storms in the region. It is also observed that the IMERG considerably overestimates the number of precipitation events with respect to the other two products; this is evident with a high POD and FAR. Regarding the relationship between the number of false alarms and the number of estimated precipitation events and the correctly estimated precipitation fraction, the CMORPH product presented the best results as indicated by the FAR and ETS indexes, respectively (Figure 8).

Tecnología y Ciencias del Agua

OPEN ACCESS

Check for updates

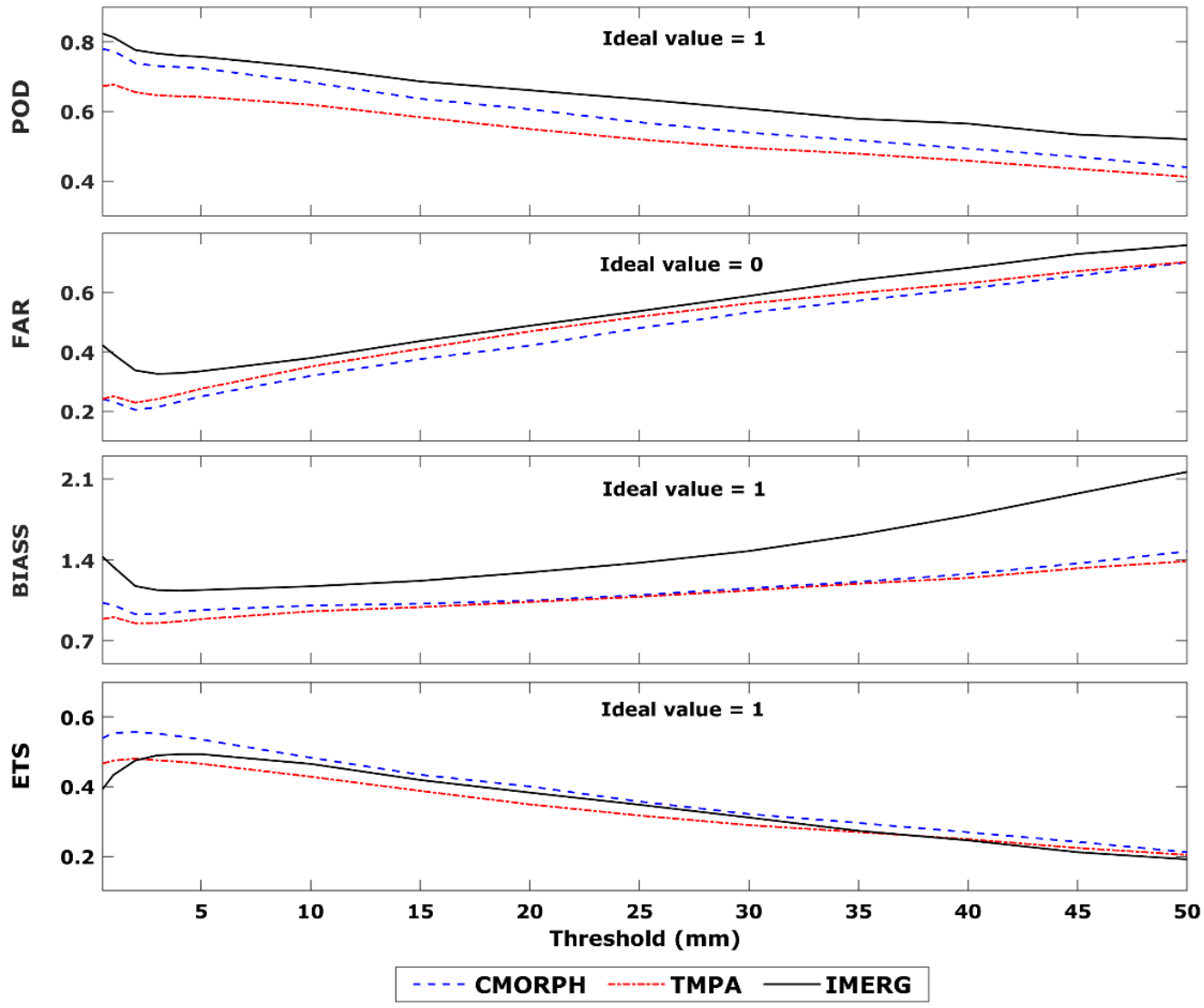


**Figure 8**. Graph of POD, FAR, BIASS and ETS based on daily precipitation thresholds. Period 2001-2017.

The impact of bias correction on SPP data was assessed using the four descriptive statistical metrics presented in Table 2. In each statistic, box diagrams were used to compare similarities in terms of symmetry, dispersion, and to determine the existence of extreme values, between the distribution of rainfall estimates and of the observed data. The results indicate that the bias removal method has satisfactorily increased the fit between SPP and surface observations as evidenced by the reduction of BIAS, RMSE and the increase in NSE and R (Figure 9).

Tecnología y Ciencias del Agua

OPEN ACCESS

Check for updates

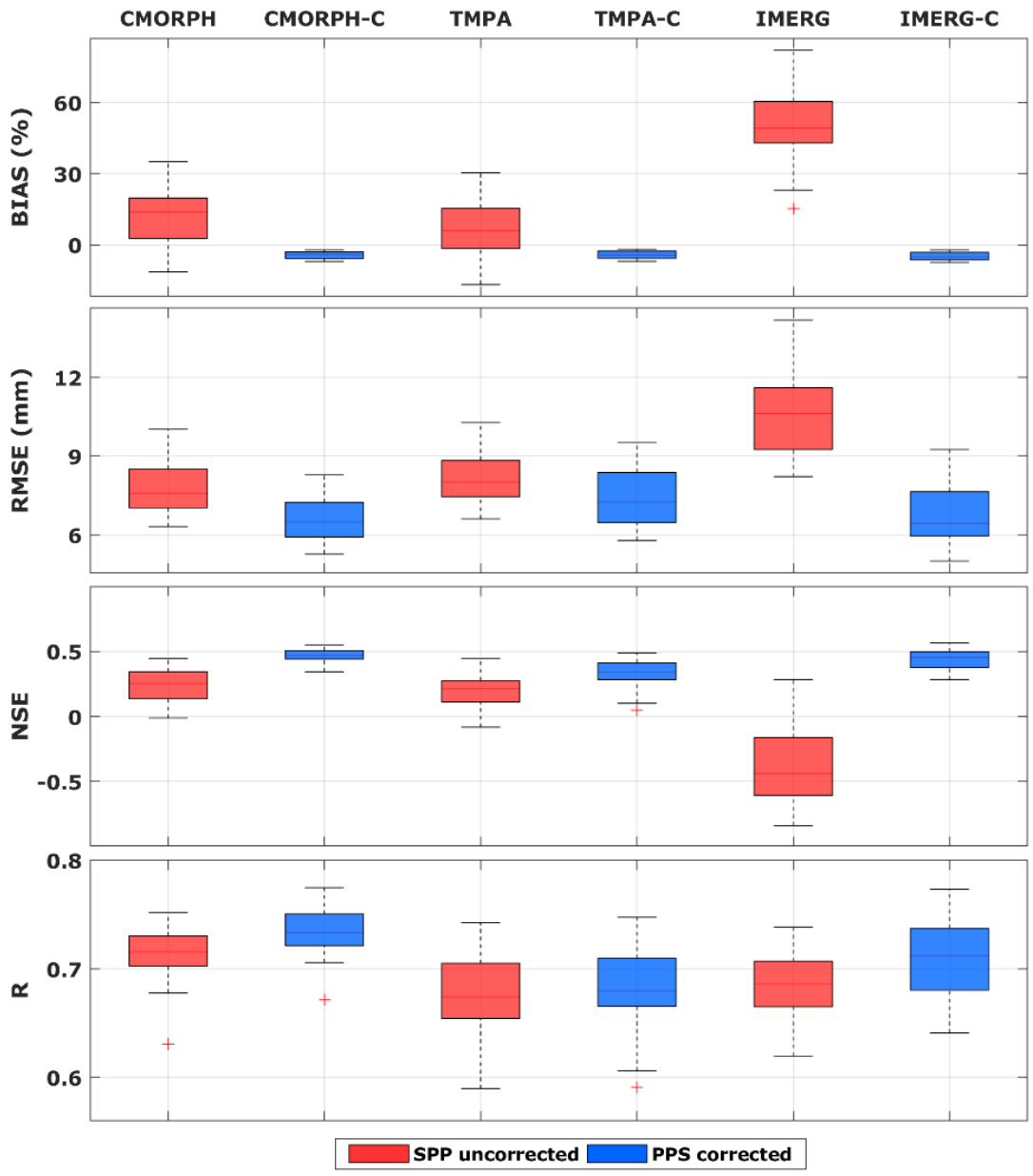

**Figure 9**. Diagram of boxes of the descriptive statistical coefficients calculated for daily rainfall. Period 2001-2017.

In the case of BIAS, it is observed that all uncorrected SPP have positive values higher than 6 %, highlighting the IMERG with a higher degree of precipitation overestimation of 53 %, on the other hand, all corrected SPPs yielded similar BIAS values, in all cases close to zero. Analyzing the results of the RMSE it was found that the corrected CMORPH product (CMORPH-C) shows the lowest total mean square error and is similar to the corrected IMERG (IMERG-C), in both cases with mean values close to 6.5 mm, while the corrected TMPA (TMPA-C) has an average value close to 7.3 mm. After performing the bias correction, a significant improvement in the NSE of the IMERG product is observed, while the CMORPH and the TMPA improve this statistic to a lesser extent, in this case the corrected products provide NSE values closer to 1, being the CMORPH-C product the one with the greatest predictive ability. The magnitude of the R in all the uncorrected SPP showed values close to 0.7; after being corrected, the products have a better fit with respect to the observed data, being the CMORPH-C product the one with the highest correlation. In general, the product CMORPH-C shows a better fit with the observations when compared with TMPA-C and IMERG-C.

Descriptive statistics for the different times of the year are shown in the box diagrams in Figure 10. In the case of bias, and analyzing first

of all the uncorrected products, it is observed for the CMORPH that the seasons of JFM and OND (warm period with the highest amount of precipitation) indicate a positive bias over 28 % on average for the 29 seasons, while the seasons of AMJ and JAS (cold period with less amount of precipitation) have a negative bias on average of 15 and 28 %, respectively. The TMPA presents a negative bias (15 %) during the season of JAS, while the IMERG presents a positive bias for all seasons of the year varying between 31 % in JAS and 76 % in AMJ, which indicates an overestimation in precipitation values. As for the BIAS behavior of the corrected SPPs, they show values close to zero in all seasons.

Tecnología y Ciencias del Agua

OPEN ACCESS

Check for updates

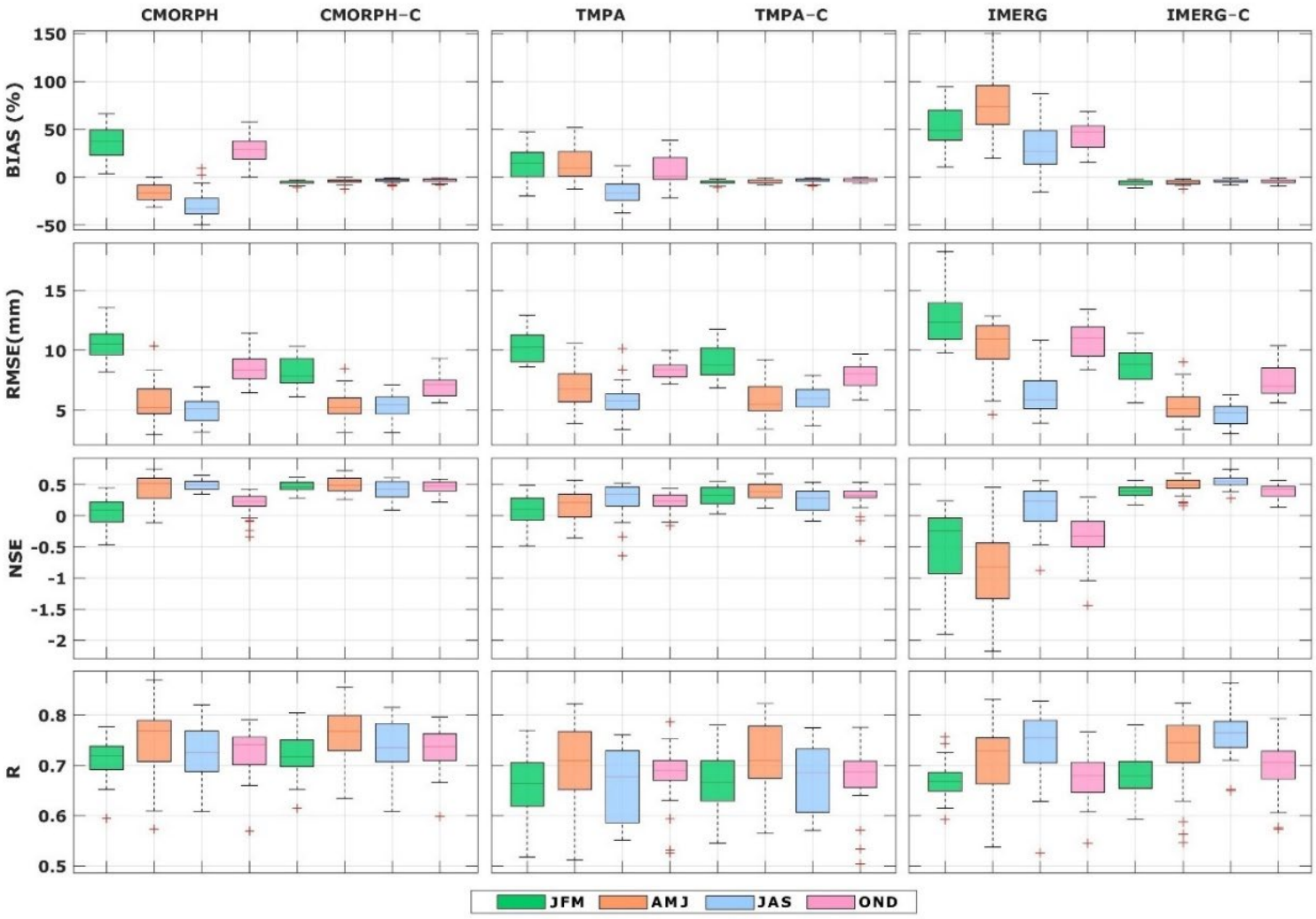


**Figure 10**. Box diagram of the descriptive statistical coefficients calculated for seasonly precipitation. Period 2001-2017.

When analyzing the results of the RMSE, it is observed that in the seasons of JFM, AMJ and OND the product that presents the least error is the CMORPH-C with daily average values of 8.1 mm; 5.4 mm and 7 mm respectively while for the months of JAS the IMERG-C product is the one that shows the best fit with an average of 4.6 mm. In the case of the NSE for each season, it was observed that in all cases the corrected SPP improve their adjustment, the behavior of the RMSE results is repeated where the CMORPH-C product better represents the seasons with the highest rainfall (JFM, AMJ and OND) with values close to 0.5; while the IMERG-C product is the one that best captures the precipitation observed for the JAS season with an average of 0.55. Finally, the R shows similar values in all SPP and when corrected they improve by about 2 %. However, values consistent with the RMSE and NSE statistics are observed since, like them, the IMERG-C product presents the highest correlation index in the JAS season, while the CMORPH-C presents a better adjustment for the rest of the seasons.

## Monthly level: pixel *vs*. pixel

The spatial distribution of the different statistics was carried out with precipitation data at the monthly level. For them, the observed precipitation data have been interpolated to the same spatial resolution of the SPP to be able to perform the evaluation pixel by pixel. Figure 11 shows the spatial distribution of BIAS for the period 2001–2017. In the JFM season where the greatest amount of precipitation is recorded, a positive BIAS is observed in most of the region, with the IMERG product being the one with the highest overestimation with an average of 60 %, while the CMORPH and TMPA products overestimate the observations, on average for the Pampean region, by 47 and 20 %, respectively.

Tecnología y Ciencias del Agua

OPEN ACCESS

Check for updates

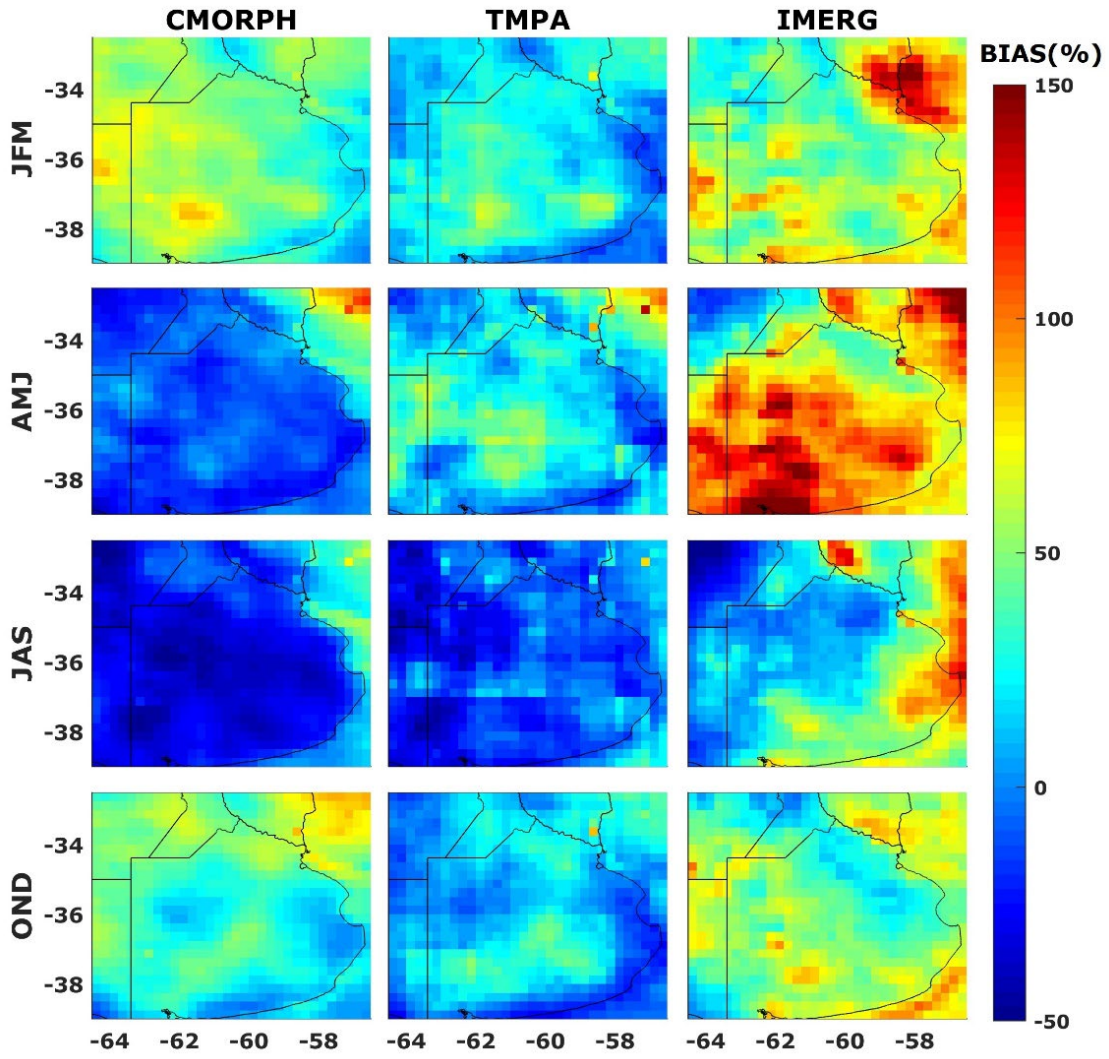


**Figure 11**. BIAS in percentage corresponding to the JFM, AMJ, JAS and OND season. Period 2001-2017.

The AMJ season shows a negative BIAS of 4 % for the CMORPH product and positives of 21 and 84 % for the TMPA and IMERG products, respectively. During the JAS season, CMORPH and TMPA products presented negative BIAS with values of 20 and 12 %. For the IMERG product it is observed that in the west of the region it presents negative values, however, the average for the whole area shows a positive BIAS of 32 %. The OND season, like the JFM season, shows a positive BIAS in the three SPP, with the IMERG product being the one with the highest overestimation with an average of 49%, the CMORPH and TMPA products overestimate the observations, by 37 and 11 %, respectively.

After having calculated the magnitude of the bias for each station (Figure 11) we proceeded to remove it using the QM method. Figure 12 shows the R between the observed data and the SPP before and after the bias correction for the different seasons analyzed. It is observed that the CMORPH-C product performs better in the JFM and AMJ seasons, with average values of 0.7 and 0.8 respectively, followed by the IMERG-C product with values of 0.69 and 0.79. As for the JAS and OND seasons, the IMERG-C product is the one with the best results with values of 0.75 and 0.73 respectively, followed by the CMORPH-C product with 0.74 in JAS and 0.70 in OND. On the other hand, in all cases the TMPA-C product presented the lowest correlations when compared with the CMORPH-C and IMERG-C products.

Tecnología y Ciencias del Agua

OPEN ACCESS

Check for updates

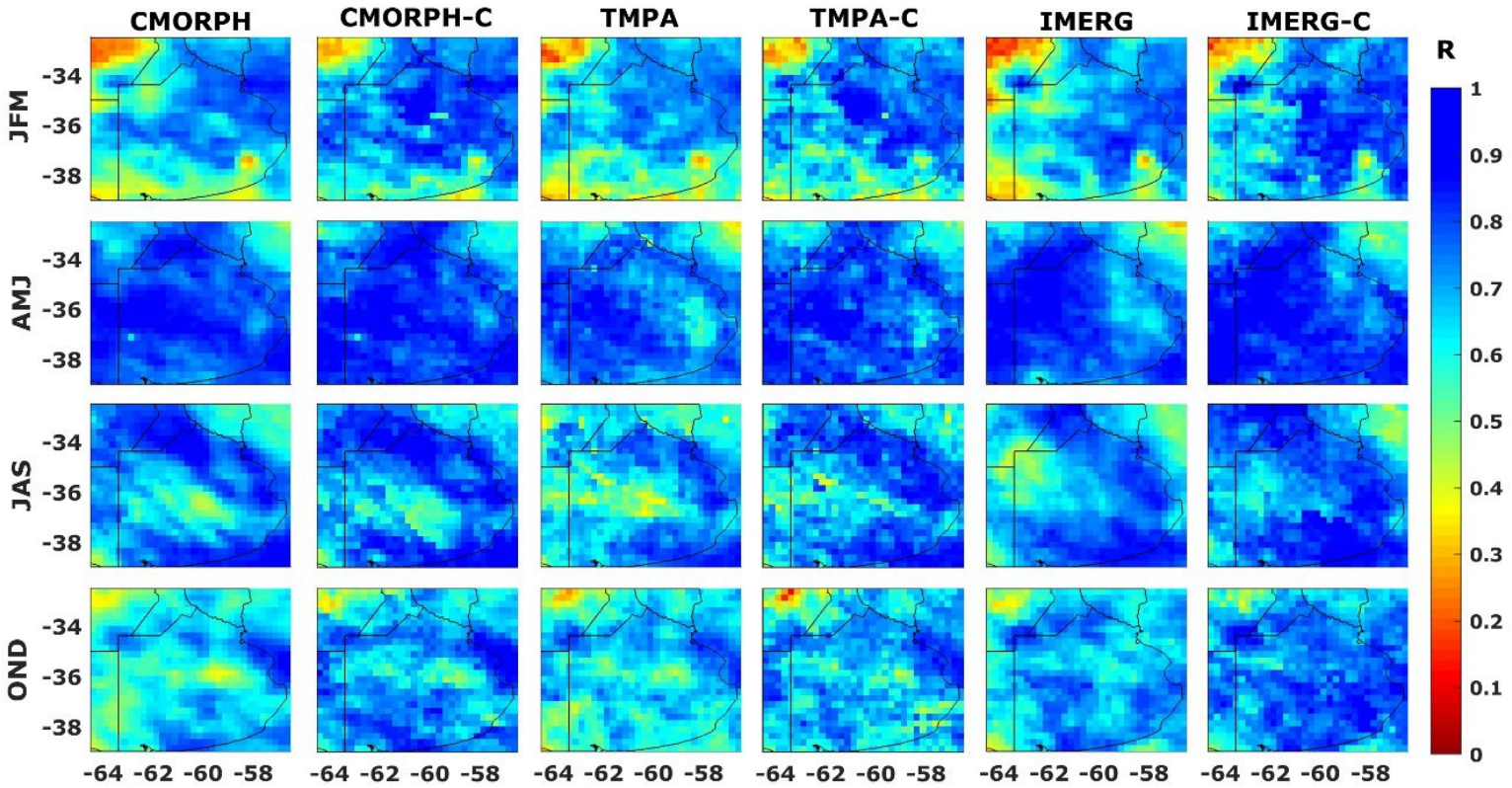


**Figure 12**. R corresponding to the JFM, AMJ, JAS and OND seasons. Period 2001-2017.

Overall, the uncorrected seasonly precipitation data of the three SPP showed good fit when compared with the observed data, the average R values vary between 0.62 and 0.78. The best settings were obtained for SPP corrected with R averages ranging from 0.67 to 0.80. This indicates

an increase in correlation between 4 and 5 % on average for the study region.

When analyzing the results for the RMSE (Figure 13), it is observed that all the corrected SPP present less error when compared with the uncorrected SPP. In general, the product with the lowest average error for the region is the IMERG-C with an average monthly value of 35 mm, then the CMORPH-C with an error of 36 mm and finally the TMPA-C with 37 mm. The errors obtained follow the same pattern with the relationships found from the R, where the CMORPH-C product presented the lowest errors in the JFM seasons with 42 mm and AMJ with 27 mm, while the JAS and OND seasons showed the lowest errors in the IMERG-C product with 29 mm and 39 mm.

Tecnología y Ciencias del Agua

OPEN ACCESS

Check for updates

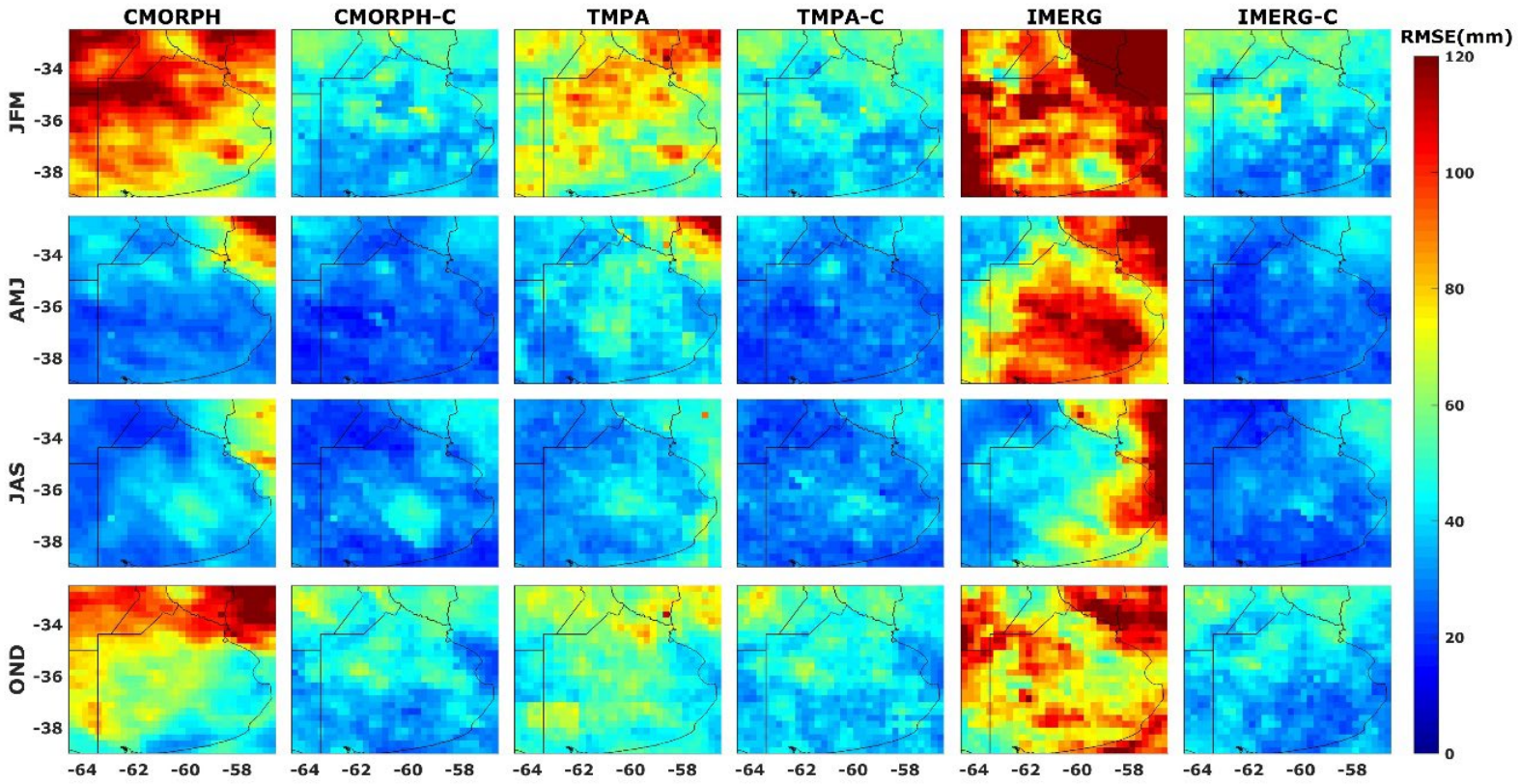


**Figure 13**. RMSE corresponding to the JFM, AMJ, JAS and OND seasons. Period 2001-2017.

Tecnología y Ciencias del Agua

OPEN ACCESS

Check for updates

# Discussion

In 1997 the TRMM satellite was launched, which was specifically designed to monitor and study tropical and subtropical rainfall, since then professionals and scientists have been evaluating the performance of precipitation estimates obtained by satellite using different algorithms (Huffman *et al*., 2007; Huffman *et al*., 2014; Joyce *et al*., 2004). These products are in different versions, those obtained near real time and those obtained later (final version). The first ones are acquired with a delay between 4 and 24 hours, and due to the immediacy in obtaining the data these products are not calibrated with precipitation on the surface. The second ones are available in different periods, which vary depending on the calibration time of the same, in some cases they are obtained 2 or 3 months after the month of the observation and are corrected with global precipitation data, for example, the IMERG product in its final version performs the correction with the analysis of the precipitation meter of the Global Precipitation Climatology Center (GPCC) (Huffman *et al*., 2014).

In order to verify the similarities and/or differences between the SPPs corrected with regional data and the SPPs in their last version calibrated with global data, the results obtained in this study were

compared with the findings of previous work (Table 3). Those where the study area was in South America with a daily time scale in different time periods were selected. Overall, the three SPP were found to correlate well in most of South America except for those evaluated in basins with complex topography (Baez-Villanueva *et al*., 2018; Hobouchian *et al*., 2017), possibly because of the lack of rainfall observations in mountainous regions.

**Table 3**. Comparison of the near real-time SPP corrected in this work with the SPP in its last version of other studies carried out on a daily scale in South America.

Tecnología y Ciencias del Agua

OPEN ACCESS

Check for updates

| Reference | Study area | Period | CMORPH | | TMPA | | IMERG | |
|---|---|---|---|---|---|---|---|---|
| | | | R | RMSE (mm/day) | R | RMSE (mm/day) | R | RMSE (mm/day) |
| This study | Argentina (Pampean region) | 01/01/2001 a 31/12/2017 | 0.73 | 6.6 | 0.68 | 7.4 | 0.73 | 6.7 |
| Salio et al., (2015) | South America | 01/12/2008 a 30/11/2010 | 0.63 | - | 0.82 | - | - | - |
| Baez-Villanueva et al., (2018) | Colombia (Magdalena Basin) | 01/01/2001 a 31/12/2014 | 0.33 | 8.8 | 0.57 | 9.0 | - | - |
| Oreggioni-Weiberlen & Báez-Benítez, (2018) | Paraguay | 1998 a 2012 | 0.45 -0.77 | 9.0 - 12.0 | 0.59 -0.77 | 7.0 - 11.0 | - | - |
| Hobouchian et al., (2017) | Chile - Argentina (subtropical Andes) | 01/01/2004 a 31/12/2010 | 0.26 | - | 0.33 | - | - | - |
| Palomino-Ángel et al., (2019) | Colombia (Biogeographic Chocó) | 2014 a 2017 | - | - | 0.31 | 15.5 | 0.41 | 14.6 |
| Nascimento et al., (2021) | Brazil (Paraná State) | 06/2000 a 12/2018 | - | - | - | - | 0.44 | 11.3 - 14.8 |

When evaluating the results of the correlation coefficient of the SPP, it is highlighted that for both the CMORPH and the IMERG the greatest similarity is the one obtained in the evaluation carried out in this study, for the case of the TMPA the best result was obtained by Salio *et al*. (2015) with an R of 0.82, however, it is necessary to mention that this considers only 2 years of records compared to the 17 years used in this analysis.

On the other hand, the three SPP corrected in this work obtained lower errors with an RMSE that varies between 6.6 and 7.4 mm/day,

compared to the results of other authors shown in Table 3. This could be related to the number of stations used in this study, where the correction was made using 29 weather stations, while the global precipitation products used to correct the SPP in their last version possibly use lower station density, which could result in biased precipitation.

This study demonstrates that the application of the QM bias correction method improves the performance of SPP to capture precipitation in the region. In addition, it allows obtaining a product near real time unlike the products in their final version that have a delay of more than a month. Likewise, carrying out a specific evaluation in each region where it is required to select a SPP is deemed necessary.

## Conclusions

The current availability of precipitation obtained through remote sensors presented the opportunity to evaluate the reliability of three SPPs (IMERG, TMPA and CMORPH) in their version in near real time, using as a reference 29 rainfall stations distributed in the Pampean region located in

southeastern Argentina. With the application of categorical and descriptive statistics, it was shown that these products tend to overestimate the amount of precipitation on a daily basis in the region.

The analysis carried out shows that the IMERG product has better capacity to detect precipitation; however, it presents a greater number of false alarms and bias. Meanwhile, the CMORPH product better represents the fraction of observed events that were correctly estimated and shows lower BIASS values for high intensities. Finally, the TMPA product is the least suitable for detecting precipitation in the region.

The incorporation of a method for removing bias in SPP, such as Quantile Mapping, introduced significant improvement in the statistics evaluated. Especially the CMORPH product exceeded its ability to detect precipitation when compared to the IMERG. After the correction of the SPP, they improve their monthly correlation between 4 and 5 %, while the daily correlation increases around 2 %. The bias correction achieved improved the quality of SPP, and consequently their use has a positive influence on different hydrometeorological applications.

The seasonly ability of the SPP with respect to weather stations showed that after bias correction the CMORPH product shows better results to represent precipitation in all seasons except the JAS season, where the IMERG product captured precipitation better. Overall, the TMPA had the least favorable performance among the SPP evaluated.

The analysis of the spatial distribution of the monthly precipitation of the observed data allowed evaluating the behavior of the SPP throughout the study area. Although the spatial mean was similar between products, the reliability of SPP varies widely within the study area. This demonstrates the importance of being able to validate and correct SPP with surface data from a network of observations dense enough to capture the spatial variability of precipitation. The CMORPH and IMERG products showed very similar performances. In the seasons of JFM and OND where most of the events come from convective phenomena and that coincides with the seasons of greater amount of precipitation, they presented greater RMSE with an average value for the region of 43 mm in the JFM season and 27 mm in OND. On the other hand, in the AMJ and JAS seasons where only 25 % of the rainfall occurs and most of these are of stratiform origin, the smallest RMSE occur with an approximate value for the region of 28 mm.

Although these satellite products have significantly improved their spatial and temporal resolution with respect to previous versions, it is necessary to deepen the evaluation of these estimates, and continue with the installation of weather stations that allow adequate monitoring of precipitation. This study could serve as a reference for researchers who wish to apply or evaluate SPP near real time to be used in hydrological applications such as flow forecasts for flood warning systems in the region.

## Acknowledgements

The authors would like to thank the CIC (Comisión de Investigaciones Científicas de la Provincia de Buenos Aires), to the National Meteorological Service of Argentina for providing data from weather stations; Eng. Ninoska Briceño for her invaluable contribution in the discussion of preliminary results.

## References

Aliaga, V. S., Ferrelli, F., & Piccolo, M. C. (2017). Regionalization of climate over the Argentine Pampas. *International Journal of Climatology*, 37(S1), 1237-1247. Recovered from https://doi.org/https://doi.org/10.1002/joc.5079

Aragón, R., Jobbágy, E. G., & Viglizzo, E. F. (2011). Surface and groundwater dynamics in the sedimentary plains of the Western Pampas (Argentina). *Ecohydrology*, 4(3), 433-447. Recovered from https://doi.org/https://doi.org/10.1002/eco.149

Aslami, F., Ghorbani, A., Sobhani, B., & Esmali, A. (2019). Comprehensive comparison of daily IMERG and GSMaP satellite precipitation products in Ardabil Province, Iran. *International Journal of Remote*

*Sensing*, 40(8), 3139-3153. Recovered from https://doi.org/10.1080/01431161.2018.1539274

Baez-Villanueva, O. M., Zambrano-Bigiarini, M., Ribbe, L., Nauditt, A., Giraldo-Osorio, J. D., & Thinh, N. X. (2018). Temporal and spatial evaluation of satellite rainfall estimates over different regions in Latin-America. *Atmospheric Research*, 213, 34-50. Recovered from https://doi.org/https://doi.org/10.1016/j.atmosres.2018.05.011

Basheer, M., & Elagib, N. A. (2019). Performance of satellite-based and GPCC 7.0 rainfall products in an extremely data-scarce country in the Nile Basin. *Atmospheric Research*, 215, 128-140. Recovered from https://doi.org/https://doi.org/10.1016/j.atmosres.2018.08.028

Borges, P. de A., Franke, J., Da-Anunciação, Y. M. T., Weiss, H., & Bernhofer, C. (2016). Comparison of spatial interpolation methods for the estimation of precipitation distribution in Distrito Federal, Brazil. *Theoretical and Applied Climatology*, 123(1-2), 335-348. Recovered from https://doi.org/10.1007/s00704-014-1359-9

Campozano, L., Sánchez, E., Avilés, Á., & Samaniego, E. (2014). Evaluation of infilling methods for time series of daily precipitation and temperature: The case of the Ecuadorian Andes. *Maskana*, 5(1 SE-Artículos científicos), 99-115. Recovered from https://doi.org/10.18537/mskn.05.01.07

Cisneros-Iturbe, H. L., Bouvier, C., & Domínguez-Mora, R. (2001). Aplicación del método kriging en la construcción de campos de tormenta en la ciudad de México. *Ingeniería Hidráulica en México*, 16(3), 5-14.

Dinku, T., Ruiz, F., Connor, S. J., & Ceccato, P. (2010). Validation and intercomparison of satellite rainfall estimates over Colombia. *Journal of Applied Meteorology and Climatology*, 49(5), 1004-1014. Recovered from https://doi.org/10.1175/2009JAMC2260.1

Ebert, E. E., Janowiak, J. E., & Kidd, C. (2007). Comparison of near-real-time precipitation estimates from satellite observations and numerical models. *Bulletin of the American Meteorological Society*, 88(1), 47-64. Recovered from https://doi.org/10.1175/BAMS-88-1-47.

Fang, G. H., Yang, J., Chen, Y. N., & Zammit, C. (2015). Comparing bias correction methods in downscaling meteorological variables for a hydrologic impact study in an arid area in China. *Hydrology and Earth System Sciences*, 19(6), 2547-2559. Recovered from https://doi.org/10.5194/hess-19-2547-2015

Fuschini-Mejía, M. C. (1994). *El agua en las llanuras.* Montevideo, Uruguay: Organización de las Naciones Unidas para la Educación, la Ciencia y la Cultura/ Oficina Regional de Ciencia y Tecnología para América Latina y el Caribe (UNESCO/ORCYT).

Gella, G. W. (2019). Statistical evaluation of high resolution satellite precipitation products in arid and semi-arid parts of Ethiopia: A note for hydro-meteorological applications. *Water and Environment Journal*, 33(1), 86-97. Recovered from https://doi.org/https://doi.org/10.1111/wej.12380

Guevara-Ochoa, C., Briceño, N., Zimmermann, E., Vives, L., Blanco, M., Cazenave, G., & Ares, G. (2017). Relleno de series de precipitación diaria para largos periodos de tiempo en zonas de llanura. Caso de estudio cuenca superior del arroyo del azul. *Geoacta (Argentina)*, 42(1), 38-60.

Heo, J. H., Ahn, H., Shin, J. Y., Kjeldsen, T. R., & Jeong, C. (2019). Probability distributions for a quantile mapping technique for a bias correction of precipitation data: A case study to precipitation data under climate change. *Water (Switzerland)*, 11(7), 1475. Recovered from https://doi.org/10.3390/w11071475

Hobouchian, M. P., Salio, P., García-Skabar, Y., Vila, D., & Garreaud, R. (2017). Assessment of satellite precipitation estimates over the slopes of the subtropical Andes. *Atmospheric Research*, 190, 43-54. Recovered from https://doi.org/https://doi.org/10.1016/j.atmosres.2017.02.006

Hong, Y., Hsu, K., Moradkhani, H., & Sorooshian, S. (2006). Uncertainty quantification of satellite precipitation estimation and Monte Carlo assessment of the error propagation into hydrologic response.

*Water Resources Research*, 42(8), W08421. Recovered from https://doi.org/https://doi.org/10.1029/2005WR004398

Hossain, F., & Anagnostou, E. N. (2004). Assessment of current passive-microwave- and infrared-based satellite rainfall remote sensing for flood prediction. *Journal of Geophysical Research: Atmospheres*, 109, D07102. Recovered from https://doi.org/https://doi.org/10.1029/2003JD003986

Hossain, F., & Anagnostou, E. N. (2006). A two-dimensional satellite rainfall error model. *IEEE Transactions on Geoscience and Remote Sensing*, 44(6), 1511-1522. Recovered from https://doi.org/10.1109/TGRS.2005.863866

Huffman, G. J., Adler, R. F., Bolvin, D. T., Gu, G., Nelkin, E. J., Bowman, K. P., Hong, Y., Stocker, E. F., & Wolff, D. B. (2007). The TRMM Multisatellite Precipitation Analysis (TMPA): Quasi-global, multiyear, combined-sensor precipitation estimates at fine scales. *Journal of Hydrometeorology*, 8(1), 38-55. Recovered from https://doi.org/10.1175/JHM560.1

Huffman, G. J., Bolvin, D. T., Braithwaite, D., Hsu, K., Joyce, R., Kidd, C., Nelkin, E. J., Sorooshian, S., Tan, J., & Xie, P. (March, 2019). *NASA Global Precipitation Measurement (GPM) Integrated Multi-satellitE Retrievals for GPM (IMERG). Algorithm Theoretical Basis Document (ATBD) Version 06*. Clear Lake, USA: National Aeronautics and Space Administration (NASA). Recovered from

https://pmm.nasa.gov/sites/default/files/document_files/IMERG_ATBD_V06.pdf

Huffman, G. J., Bolvin, D. T., Braithwaite, D., Hsu, K., Joyce, R., & Xie, P. (2014). *NASA Global Precipitation Measurement (GPM) Integrated Multi-satellitE Retrievals for GPM (IMERG). Algorithm Theoretical Basis Document (ATBD) Version 4.4*. Clear Lake, USA: National Aeronautics and Space Administration (NASA). Recovered from https://pmm.nasa.gov/sites/default/files/document_files/IMERG_ATBD_%0AV4.4.pdf.

Iida, Y., Kubota, T., Iguchi, T., & Oki, R. (2010). Evaluating sampling error in TRMM/PR rainfall products by the bootstrap method: Estimation of the sampling error and its application to a trend analysis. *Journal of Geophysical Research: Atmospheres*, 115, D22119. Recovered from https://doi.org/https://doi.org/10.1029/2010JD014257

Ines, A. V. M., & Hansen, J. W. (2006). Bias correction of daily GCM rainfall for crop simulation studies. *Agricultural and Forest Meteorology*, 138(1-4), 44-53. Recovered from https://doi.org/10.1016/j.agrformet.2006.03.009

Joyce, R. J., Janowiak, J. E., Arkin, P. A., & Xie, P. (2004). CMORPH: A method that produces global precipitation estimates from passive microwave and infrared data at high spatial and temporal resolution. *Journal of Hydrometeorology*, 5(3), 487-503. Recovered

from https://doi.org/10.1175/1525-7541(2004)005<0487:CAMTPG>2.0.CO;2

Kim, J., & Ryu, J. H. (2016). A heuristic gap filling method for daily precipitation series. *Water Resources Management*, 30(7), 2275-2294. Recovered from https://doi.org/10.1007/s11269-016-1284-z

Luo, M., Liu, T., Meng, F., Duan, Y., Frankl, A., Bao, A., & De-Maeyer, P. (2018). Comparing bias correction methods used in downscaling precipitation and temperature from regional climate models: A case study from the Kaidu River Basin in Western China. *Water (Switzerland)*, 10(8), 1-21. Recovered from https://doi.org/10.3390/w10081046

Maggioni, V., & Massari, C. (2018). On the performance of satellite precipitation products in riverine flood modeling: A review. *Journal of Hydrology*, 558, 214-224. Recovered from https://doi.org/https://doi.org/10.1016/j.jhydrol.2018.01.039

Magrin, G. O., Travasso, M. I., López, G. M., Rodriguez, G. R., & Lloveras, A. R. (2007). Vulnerabilidad de la producción agrícola en la región pampeana argentina. In: *Componente B3 de la 2da Comunicación Nacional de Cambio Climático*. Recovered from http://climayagua.inta.gob.ar/sites/default/files/cambiocli/Vulnerabilidad_Produccion_Agricola_Region_Pampeana.pdf

Melo, D. de C. D., Xavier, A. C., Bianchi, T., Oliveira, P. T. S., Scanlon, B. R., Lucas, M. C., & Wendland, E. (2015). Performance evaluation of rainfall estimates by TRMM Multi-satellite Precipitation Analysis 3B42V6 and V7 over Brazil. *Journal of Geophysical Research: Atmospheres*, 120(18), 9426-9436. Recovered from https://doi.org/https://doi.org/10.1002/2015JD023797

Nascimento, J. G., Althoff, D., Bazame, H. C., Neale, C. M. U., Duarte, S. N., Ruhoff, A. L., & Gonçalves, I. Z. (2021). Evaluating the latest imerg products in a subtropical climate: The case of paraná state, brazil. *Remote Sensing*, 13(5), 1-20. Recovered from https://doi.org/10.3390/rs13050906

Oreggioni-Weiberlen, F., & Báez-Benítez, J. (2018). Assessment of satellite-based precipitation estimates over Paraguay. *Acta Geophysica*, 66(3), 369-379. Recovered from https://doi.org/10.1007/s11600-018-0146-x

Palharini, R. S., Vila, D. A., Rodrigues, D. T., Quispe, D. P., Palharini, R. C., de Siqueira, R. A., & de Sousa Afonso, J. M. (2020). Assessment of the extreme precipitation by satellite estimates over South America. *Remote Sensing*, 12(13), 2085. Recovered from https://doi.org/10.3390/rs12132085

Palomino-Ángel, S., Anaya-Acevedo, J. A., & Botero, B. A. (2019). Evaluation of 3B42V7 and IMERG daily-precipitation products for a very high-precipitation region in northwestern South America.

*Atmospheric Research*, *217*, 37-48. Recovered from https://doi.org/10.1016/j.atmosres.2018.10.012

Salio, P., Hobouchian, M. P., García-Skabar, Y., & Vila, D. (2015). Evaluation of high-resolution satellite precipitation estimates over southern South America using a dense rain gauge network. *Atmospheric Research*, 163, 146-161. Recovered from https://doi.org/https://doi.org/10.1016/j.atmosres.2014.11.017

Tan, M. L., & Duan, Z. (2017). Assessment of GPM and TRMM Precipitation Products over Singapore. *Remote Sensing*, 9(7), 720. Recovered from https://doi.org/10.3390/rs9070720

Tan, M. L., & Santo, H. (2018). Comparison of GPM IMERG, TMPA 3B42 and PERSIANN-CDR satellite precipitation products over Malaysia. *Atmospheric Research*, 202, 63-76. Recovered from https://doi.org/https://doi.org/10.1016/j.atmosres.2017.11.006

Tang, L., & Hossain, F. (2009). Transfer of satellite rainfall error from gaged to ungaged locations: How realistic will it be for the Global Precipitation Mission? *Geophysical Research Letters*, 36(10), L10405. Recovered from https://doi.org/https://doi.org/10.1029/2009GL037965

Tang, L., Hossain, F., & Huffman, G. J. (2010). Transfer of satellite rainfall uncertainty from gauged to ungauged regions at regional and seasonal time scales. *Journal of Hydrometeorology*, 11(6), 1263-1274. Recovered from https://doi.org/10.1175/2010JHM1296.1

Themeßl, M. J., Gobiet, A., & Heinrich, G. (2012). Empirical-statistical downscaling and error correction of regional climate models and its impact on the climate change signal. *Climatic Change*, 112(2), 449-468. Recovered from https://doi.org/10.1007/s10584-011-0224-4

Villarini, G., Mandapaka, P. V., Krajewski, W. F., & Moore, R. J. (2008). Rainfall and sampling uncertainties: A rain gauge perspective. *Journal of Geophysical Research Atmospheres*, 113(11), D11102. Recovered from https://doi.org/10.1029/2007JD009214

Yilmaz, K. K., Hogue, T. S., Hsu, K., Sorooshian, S., Gupta, H. V, & Wagener, T. (2005). Intercomparison of rain gauge, radar, and satellite-based precipitation estimates with emphasis on hydrologic forecasting. *Journal of Hydrometeorology*, 6(4), 497-517. Recovered from https://doi.org/10.1175/JHM431.1

Zambrano-Bigiarini, M., Nauditt, A., Birkel, C., Verbist, K., & Ribbe, L. (2017). Temporal and spatial evaluation of satellite-based rainfall estimates across the complex topographical and climatic gradients of Chile. *Hydrology and Earth System Sciences*, 21(2), 1295-1320. Recovered from https://doi.org/10.5194/hess-21-1295-2017